A Model of Electric Field Assisted Capillarity for the Fabrication of Hollow Microstructures

Catherine E. H. Tonry*[1], Mayur K. Patel[1], Chris Bailey[1], and Marc P. Y. Desmuliez[2]
[1]Univeristy of Greenwich, [2]Heriott Watt University
*Corresponding author: School of Computing and Mathematical Sciences, University of Greenwich, Park Row, Greenwich, London, SE10 9LS, Email: C.E.Tonry@Greenwich.ac.uk

Abstract: Electric Field Assisted Capillarity (EFAC) is a novel technique for the fabrication of hollow polymer microstructures. It has advantages over current methods as it is a single step process. Hollow microstructures have many uses in industry from microchannels and microcapsules in BioMEMS to fibre-optical waveguides. It makes use of the dielectric properties of polymers combined with a heavily wetted surface to produce fully enclosed microstructures. A model has been developed in COMSOL 4.2 to look at the complex interactions of the forces involved. The model is a fully coupled model combining both the electrostatics and phase-field modules within COMSOL. Results from the simulations agree with the experimental data available and have suggested several further avenues for experimental study.

Keywords: Microstructures, Microfluidics, CFD, Capillarity, Polymers

1. Introduction

Electric Field Assisted Capillarity (EFAC) is a novel method for the fabrication of hollow polymer microstructures[1]. It in itself is an extension of Electrohydrodynamic Induced Patterning (EHDIP), which is known in most literature as Lithographically Induced Self-Assembly (LISA)[2] though as it is neither a lithographic or self-assembly process this term will not be used here.

EFAC is driven by both dielectric and capillary forces to create fully enclosed polymer microstructures. The process works with a molten polymer placed between two electrodes. (Fig. 1) The two driving forces are concentrated at the interface between the polymer and the other fluid, usually air but any dielectric fluid should work, and are balanced primarily by the pressure caused by encapsulating this fluid within the polymer.

The process starts out with a bottom electrode spin coated with a thin film of a molten polymer and a shaped top electrode (a) when a potential is applied between these two electrodes the dielectric forces on the surface of the polymer cause the surface to grow up towards the top electrode under the lower parts of this

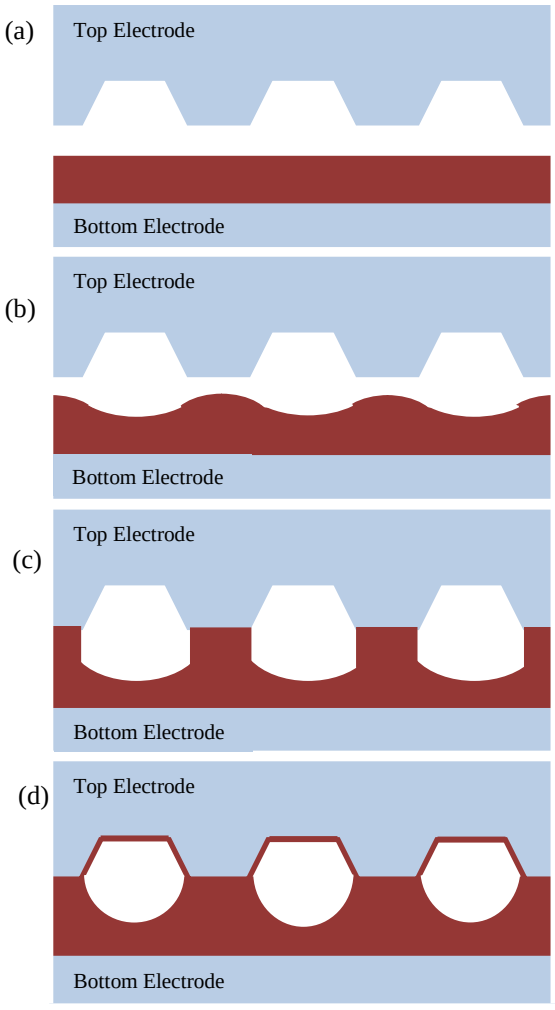

Figure 1. Schematic of the Electric Field Assisted Capillarity (EFAC) process. The dark (red) region is the polymer.

electrode (b) Eventually the polymer reaches the top electrode (c) at this point due to the heavily wetted top surface, with a contact angle in the

range of approximately ten to thirty degrees causes the polymer to completely coat the top mask forming a fully enclosed microstructure. The process has been shown to work on a scale of a few microns to a few hundred microns, however theoretically it should also work on a nanoscale provided that suitable masks can be produced.

2. Governing Equations

The initial driving force on the polymer is the dielectric force at the interface between the two fluid. This force, which is concentrated at the interface between the two fluids, can be calculated from the equation for the force on a dielectric[3]:

$$\mathbf{F} = \rho_f \mathbf{E} - \frac{1}{2}\mathbf{E}\cdot\mathbf{E}\nabla\epsilon + \nabla\left(\frac{1}{2}\mathbf{E}\cdot\mathbf{E}\frac{\partial\epsilon}{\partial\rho}\rho\right) \quad \text{Eq. 1}$$

The first term in this equation is the electrostatic force due to a charge density ρ_f. The second term is due to inhomogeneities in the dielectric constant, as both fluids are considered to have a uniform dielectric constant this only has a value at the interface. The final term is the electrostriction force density this comes from changes in the materials mass density as both fluids are assumed to be incompressible this only has a value at the interface.

The polymer is assumed to be a perfect dielectric it therefore has zero free charge in the bulk material however there will be a charge at the interface due to the change in the dielectric, this can be calculated as[4]:

$$\sigma = (\epsilon_r - 1)\epsilon_0\,\mathbf{E}\cdot\hat{\mathbf{n}} \quad \text{Eq. 2}$$

This equation is a surface charge density and is therefore an area density; ρ_f is however a volume density and so to obtain this the gradient of the free surface variable can be used in place of the unit normal at the interface.

$$\rho_f = (\epsilon_r - 1)\epsilon_0\,\mathbf{E}\cdot\nabla\phi \quad \text{Eq. 3}$$

This gives the overall equation for the dielectric force density at the interface as:

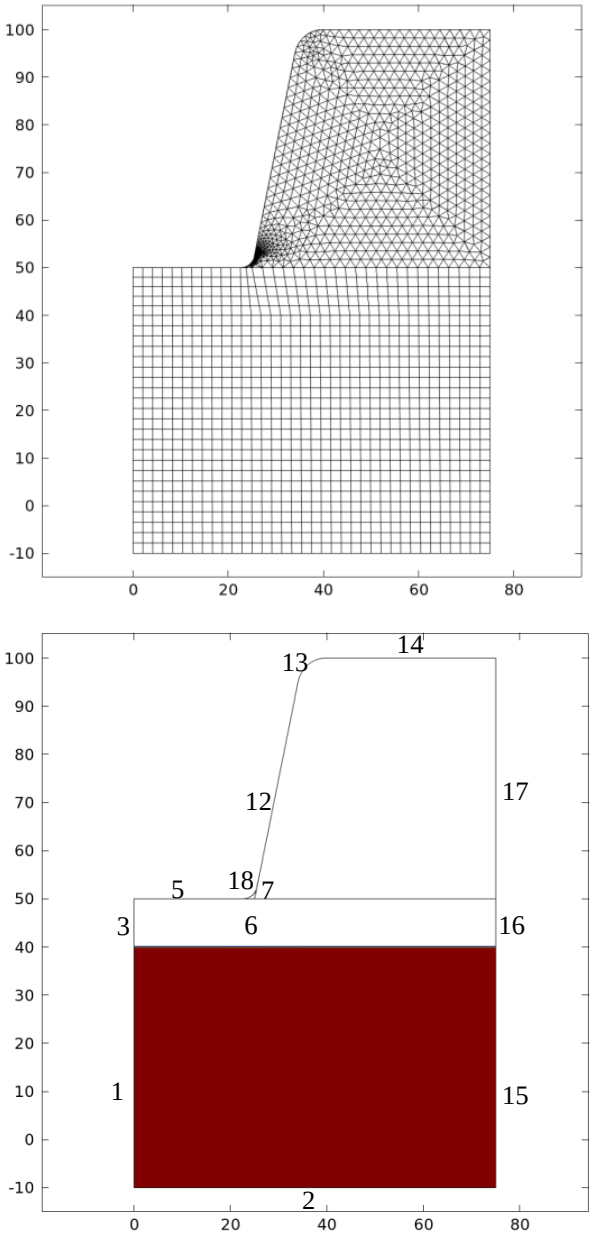

	Flow	Electric Field
1	Slip Wall	Symmetry
2	No-Slip Wall	0V
3	Slip wall	Symmetry
5	Slip wall	300V
6	Wetted Wall	N/A
7	Wetted Wall	N/A
12	Wetted Wall	300V
13	Wetted Wall	300V
15	Symmetry	Symmetry
16	Symmetry	Symmetry
17	Symmetry	Symmetry
18	N/A	300V

Figure 2. Mesh, Geometry and Boundary Conditions

$$\mathbf{F} = ((\epsilon_r - 1)\epsilon_0\,\mathbf{E}\cdot\nabla\phi)\mathbf{E} - \frac{1}{2}\mathbf{E}\cdot\mathbf{E}\nabla\epsilon + \nabla\left(\frac{1}{2}\mathbf{E}\cdot\mathbf{E}\frac{\partial\epsilon}{\partial\rho}\rho\right) \quad \text{Eq. 4}$$

The remainder of the governing equations are the defaults used within COMSOL.

3. Use of COMSOL Multiphysics

COMSOL Multiphysics 4.0 was used to set up the original model however it was upgraded to 4.2 for the later results. The model is two dimensional representing an infinitely long microchannel, the symmetry of the problem has also been exploited.

The Electrostatics and Incompressible Phase Field modules were used to model the physics. These were coupled together using the governing equation for the force at the interface listed previously. However there was an issue with implementing this equation directly as for some reason when used in a variable the components of the electric field evaluated to zero, therefore the spatial gradient of the voltage was used in its place.

The electrostatics module was used with zero free charge as both the air and the polymer were assumed to be perfect dielectrics. The Boundary conditions were a high voltage on the top mask, ground on the bottom mask and symmetry (zero charge) at the sides of the mask these can be seen in Fig. 2.

The phase field module was used rather than the level set for two reasons. Firstly the phase field tends to be more stable for surface tension for small scales and secondly it will make it easier to implement the viscoelastic elements of the problem at a later date. The polymer is currently modeled as a Newtonian fluid however in future this will need changing to consider the effects of the viscoelastic properties of the polymer.

The boundary conditions here were a heavily wetted wall on the top mask, a no slip wall on the bottom mask and symmetry at the sides these can again be seen in Fig. 2.

A mapped mesh was used for the two Lower regions of the mask and a free triangular mesh used for the top part of the mask, this mesh can be seen in Fig. 2. This is the mesh for the geometry of the results presented here, other meshes have also been used to simulate different geometries of different shaped microchannels.

The material properties were that of Polydimethylsiloxane (PDMS) with the exception of the viscosity where an artificially lower viscosity was used to enable the simulation to run in a lower timescale. This was necessary as with the higher viscosity the simulations timestep needed to be too large for the phase field model and so mass was not

Simulation Dynamic Viscosity (Centipoise)	Specific Gravity (25°C)	Dielectric Constant(100 Hz)	Surface Tension (mN/m)
1000	1.03	2.72	20

Figure 3. Material Properties of PDMS

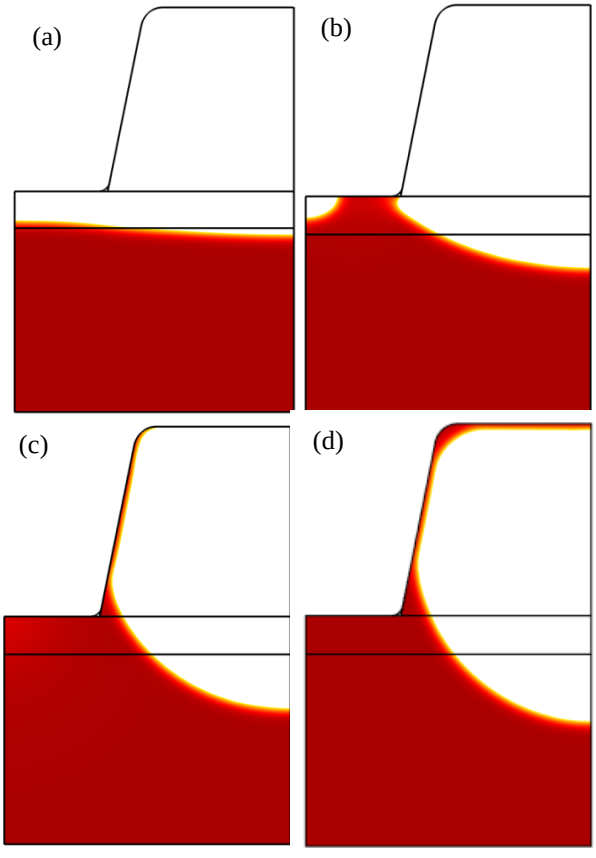

Figure 4. Evolution of the polymer surface over time

conserved. The properties used can be seen in Fig. 3.

The material properties use for air were the properties from the COMSOL materials library.

4. Results

The results for the geometry in Fig. 2 can be seen in Fig. 4. These is for a contact angle of 20 degrees on the wetted top mask. The force on the fluid is greater under the profusion of the mask due to the increased electric field, this causes the polymer to flow upwards at these points (a). When the polymer reaches the top mask (b) the surface tension becomes dominant, about an order of magnitude greater than the dielectric forces, this causes the fluid to flow up the mask reaching the corner (c) this continues reaching the middle of the channel and a steady state thus coating the mask (d). This is the general evolution of the flow for complete cases.

The evolution of the voltage (colour) and electric field (streamlines) for the same timesteps as Fig. 4 can be seen in Fig. 5. The higher electric field at the surface under the protrusion in the mask can be seen in these images. Also of note is the changing electric field.

Fig. 6 shows a comparison of the same geometry but differing contact angles. From these results the contact angle seems to have an effect on the final thickness of the shell; with a lower contact angle causing a thicker shell to form. If the

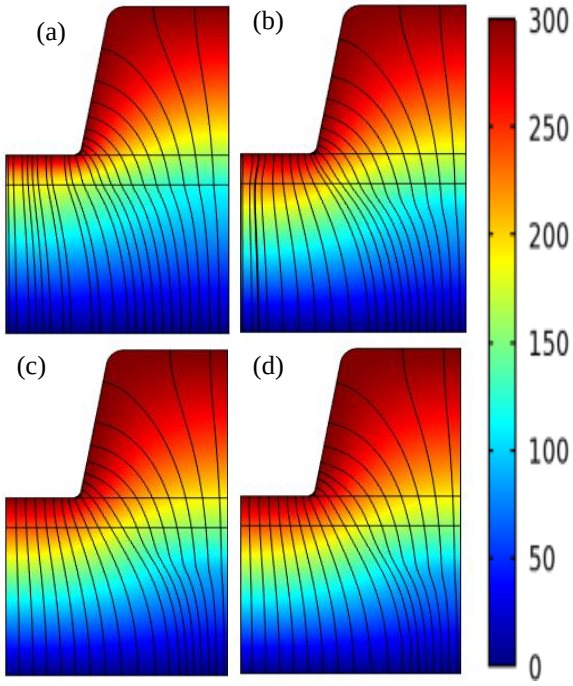

Figure 5 Evolution of the Electric field over time

contact angle becomes too large then an incomplete cap is formed. It is thought that this is due to the capillary force being insufficient to do so.

The surface is thinner in certain places and this could potentially cause problems. The electron micrograph image of the square capsules in Fig. 7 show similar thin areas though this is for a capsule rather than a channel these areas of thinness are where these capsules have 'failed'

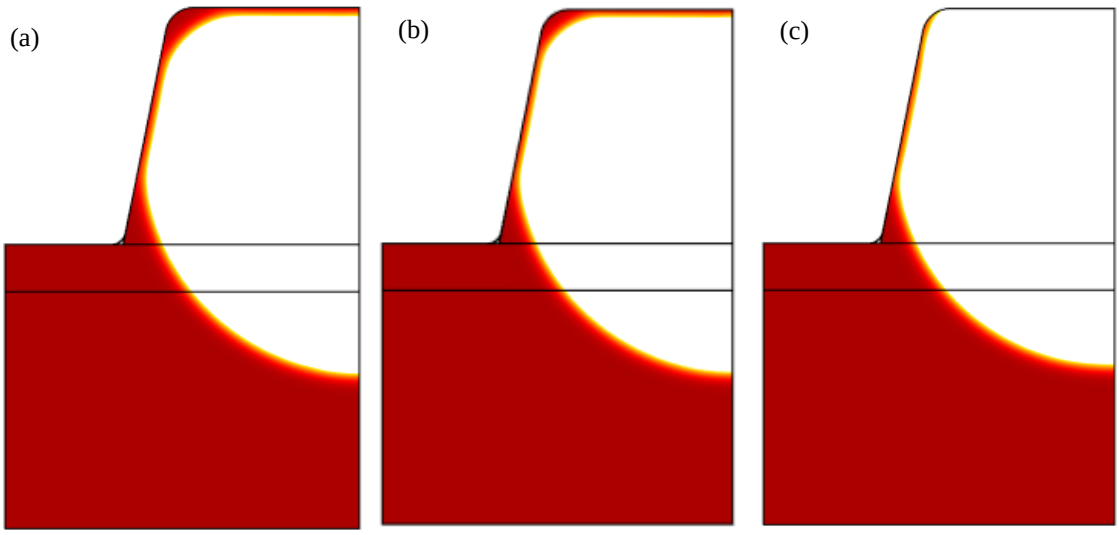

Figure 6 Comparison of the structures formed by different contact angles for the top mask (a) 10 Degrees, (b) 20 Degrees and (c) 25 Degrees

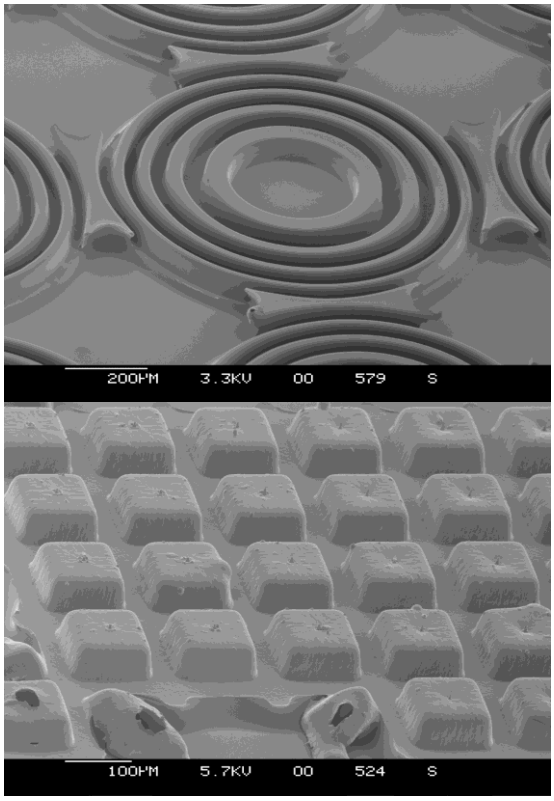

Figure 7 Electron Micrograph Image of a circular array of angled microchannels and square capsules

and have holes in them, both at the top and on the side.

Fig. 8 demonstrates a channel with a larger air gap. This had the same amount of polymer as the other results however the air gap was increased. As can be seen from these results this just creates a larger channel for the same amount of material. Also of note here is that a wetted surface was also used for the bottom boundary thus causing a thin coating at the bottom as well as the top.

Simulations have been undertaken with removing the electric field after the polymer reaches the top mask. These simulations show that the electric field is not necessarily needed at this point as the capillary force is dominant anyway.

Simulations have also been undertaken that demonstrate that changing the voltage will have an effect the speed of the first stage of the process, where the electric force is dominant.

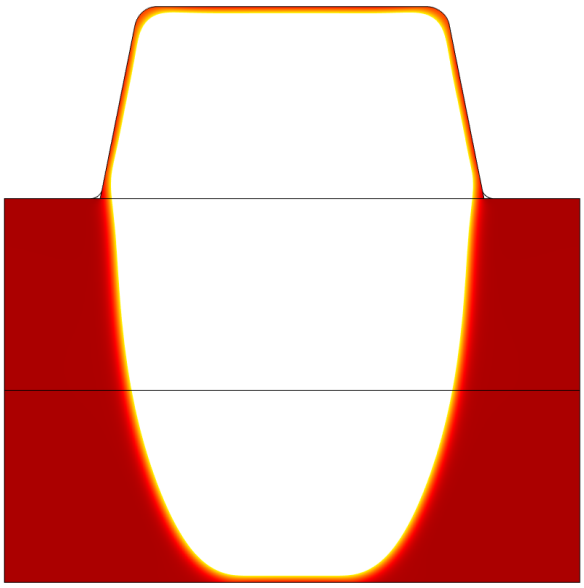

Figure 8 A channel with a 50 µm air gap

However very little effect on the second stage, where the capillary force is dominant. This has the effect of speeding up the overall process as the first stage takes a lot longer than the second stage.

5. Conclusions

The model described here has been implemented and shown to give similar results to experimental data available. However there is currently limited quantities of this data and what is available is just images of the channels formed. This means that the model has been difficult to fully validate. In order to validate the model an analytic solution to a steady state of a cylindrical channel is currently being worked on.

In addition to a validation of the model several further aspects of the physics need to be considered. The first of these is that the fact that the Non-Newtonian nature of the polymer has not currently been considered and it is assumed to be Newtonian, for more accurate results this will need implementing into the model. Secondly currently the fact that surface tension properties of materials are modified by electric fields is currently not implemented within the model so this will need to be considered in a more refined version. Finally the model needs expanding into 3 dimensions so a greater range of structures can be looked out, this should not be an issue other that simulation time.

8. References

1. H. Chen, W. Yu, S. Cargill, M. K. Patel, C. Bailey, C. Tonry and M. P. Y. Desmulliez, Self-encapsulated hollow microstructures formed by electric field-assisted capillarity, *Microfluidics and Nanofluidics*, **Volume 13**, Number 1, 75-82 (2012)

2. S. Y Chou and L. Zhuang, Lithographically induced self-assembly of periodic polymer micropillar arrays., *Papers from the 43rd international conference on electron, ion, and photon beam technology and nanofabrication*, Volume 17(6), 3197-3202, 1999

3. H. H. Woodson and J. R. Melcher, *Electromechanical Dynamics, Vol 3: Elastic and Fluid Media;* Wiley & Sons: New York, 1968

4. I.S. Grant and W.R. Philips, *Electromagnetism (Second Edition)*, John Wiley & Sons(Sussex, 1990), pp. 50-70.